ECOLOGY

Small-molecule mimicry hunting strategy in the imperial cone snail, *Conus imperialis*

Joshua P. Torres[1], Zhenjian Lin[1]*, Maren Watkins[2], Paula Flórez Salcedo[3], Robert P. Baskin[2], Shireen Elhabian[4], Helena Safavi-Hemami[2,5,6], Dylan Taylor[2], Jortan Tun[2], Gisela P. Concepcion[7], Noel Saguil[1], Angel A. Yanagihara[8], Yixin Fang[1], Jeffrey R. McArthur[9], Han-Shen Tae[9], Rocio K. Finol-Urdaneta[9], B. Duygu Özpolat[10], Baldomero M. Olivera[2], Eric W. Schmidt[1,2]*

Venomous animals hunt using bioactive peptides, but relatively little is known about venom small molecules and the resulting complex hunting behaviors. Here, we explored the specialized metabolites from the venom of the worm-hunting cone snail, *Conus imperialis*. Using the model polychaete worm *Platynereis dumerilii*, we demonstrate that *C. imperialis* venom contains small molecules that mimic natural polychaete mating pheromones, evoking the mating phenotype in worms. The specialized metabolites from different cone snails are species-specific and structurally diverse, suggesting that the cones may adopt many different prey-hunting strategies enabled by small molecules. Predators sometimes attract prey using the prey's own pheromones, in a strategy known as aggressive mimicry. Instead, *C. imperialis* uses metabolically stable mimics of those pheromones, indicating that, in biological mimicry, even the molecules themselves may be disguised, providing a twist on fake news in chemical ecology.

INTRODUCTION

Cone snails are among the most diverse groups of shelled mollusks, in part because of their prey specialization on fish, worms, or other mollusks (*1*). The main tool used for predation is a specialized organ, the venom gland. This gland synthesizes a complex mixture of bioactive molecules, the conopeptides or conotoxins, which are injected into prey through a harpoon-like radula. Because many conopeptides from fish-feeding cones target vertebrate ion channels and receptors with exquisite selectivity, they have been an exceptional source of pharmaceuticals and pharmaceutical leads, including a U.S. Food and Drug Administration (FDA)–approved pain drug (*2*–*4*).

Piscivorous cone snails have adopted at least three complex behavioral strategies to hunt highly mobile fish prey (*5*). For example, some fish hunters use "net engulfment," in which multiple fish are engulfed in the snail's mouth, which adopts a net-like structure. There, the fish relax, probably due to components released into the water, and are subsequently stung and consumed one at a time. One relaxant peptide is a fast-acting, weaponized insulin, which causes hypoglycemia in prey (*6*, *7*). Venom insulin results from duplication of the normal mollusk insulin and diversification to structurally mimic fish insulin, but in a form that evades the normal metabolic control of insulin action (*8*). The same insulins used to quiet fish prey have potential as leads for treating diabetes (*9*). Thus, there is a relationship between the hunting strategy and the potential medical application of cone snail venom peptides (*10*).

By contrast, much less is known about the behaviors of worm-hunting cone snails, although these snails make up the vast majority of cones. Worm hunters also produce conopeptides with biomedical potential (*11*), including ImI from *Conus imperialis* (*12*), implying that a better understanding of their hunting strategies might similarly aid drug discovery. The *C. imperialis* venom gland is divided into a section that is proximal to the bulb, a muscular organ responsible for ejecting venom, and a darkly colored red or greenish distal section adjacent to the harpoon. In a recent advance, we showed that conopeptides such as ImI are found in the proximal gland, while the colored distal venom is composed instead of small molecules (*13*). The first of these to be characterized more than 20 years ago was the neurotransmitter serotonin (*14*), while more recently we described genuanine, a compound so far found only in *C. imperialis* and *Conus genuanus* (*13*). We hypothesized that, in analogy to the better-known conopeptides, these small molecules contribute to prey capture.

Here, we show that the small molecules found in the *C. imperialis* venom gland are deployed as part of a complex worm-hunting behavioral strategy (Fig. 1). We define the chemical structures of several unique small molecules from the *C. imperialis* venom gland and demonstrate that the compounds act as metabolically stable mimics of prey pheromones. The major compounds, conazoliums A and B, are synthesized by epithelial cells in the venom gland. We show that diverse, bioactive small molecules are present in the colored portion of the glands and provide video evidence that the colored venom is injected into prey polychaetes. In a model polychaete, the compounds induce mating behaviors, revealing that they act as pheromones in the predatory strategy. This work demonstrates a role for small molecules in the cone snail venom, reveals that these compounds are structurally diverse yet species specific in distribution, and unveils a complex prey capture strategy in cones.

RESULTS

Small-molecule chemistry of *C. imperialis* venom glands

C. imperialis specimens were collected in the Philippines, Hawaii, Taiwan, Vanuatu, and Papua New Guinea (table S1). Distal venom gland metabolomes from the Philippines and Hawaii were analyzed. A chemistry-first approach led to the isolation and nuclear magnetic

[1]Department of Medicinal Chemistry, College of Pharmacy, University of Utah, Salt Lake City, UT 84112, USA. [2]School of Biological Sciences, University of Utah, Salt Lake City, UT 84112, USA. [3]Department of Neurobiology and Anatomy, University of Utah, Salt Lake City, UT 84112, USA. [4]Scientific Computing and Imaging Institute, School of Computing, University of Utah, Salt Lake City, UT 84112, USA. [5]Department of Biomedical Sciences, University of Copenhagen, Copenhagen DK-2200, Denmark. [6]Department of Biochemistry, University of Utah, Salt Lake City, UT 84112, USA. [7]Marine Science Institute, University of the Philippines, Diliman, Quezon City 1101, Philippines. [8]Department of Tropical Medicine, University of Hawaii, Honolulu, HI 96822, USA. [9]Illawarra Health and Medical Research Institute, University of Wollongong, Wollongong, NSW 2522, Australia. [10]Marine Biological Laboratory, Woods Hole, MA 02543, USA.
*Corresponding author. Email: ews1@utah.edu (E.W.S.); z.j.lin@utah.edu (Z.L.)

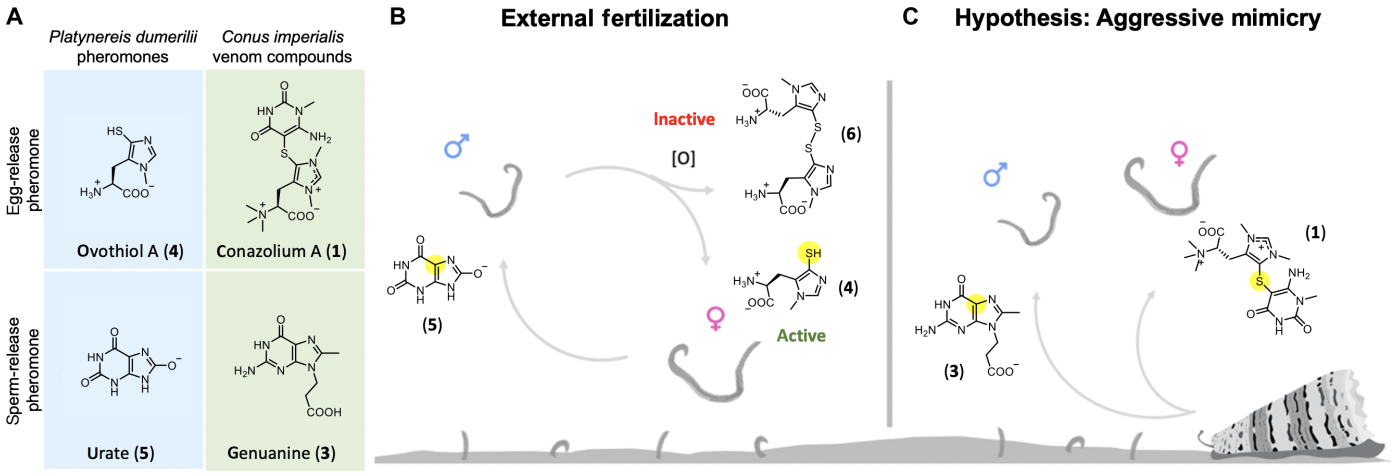

Fig. 1. Small-molecule mimicry hunting strategy of *C. imperialis*. (**A**) Conazolium A and genuanine are major small-molecule components of *C. imperialis* venom that mimic the pheromones used by sexually mature marine polychaetes in mating. (**B**) Male *P. dumerilii* releases ovothiol A to induce female worms to release eggs along with uracil. Male worm senses uracil and responds by releasing sperm to complete the external fertilization process. (**C**) A proposed model on aggressive mimicry: *C. imperialis* hijacks the mating process by releasing conazolium A and genuanine to lure and capture worms through initiation of the mating process.

resonance (NMR)–based characterization of two previously undescribed compounds, conazoliums A (**1**) and B (**2**), as well as the known genuanine (**3**) (*13*), as the major compounds present in the distal venom glands. The structures of conazoliums were elucidated using spectroscopy and chemical degradation.

Conazolium A (**1**) was isolated as its trifluoroacetate salt. The molecular formula $C_{16}H_{25}N_6O_4S^+$ was assigned on the basis of a molecular ion at mass/charge ratio (*m*/*z*) 397.1643 and the ^1H and ^{13}C NMR spectra (table S2 and fig. S1). The presence of the histidinyl moiety could be inferred from heteronuclear multiple bond correlation (HMBC) crosspeaks (fig. S1). This moiety was attached via a thioether bond to another functional group, which based on the remaining formula of $C_5H_6N_3O_2$, an ultraviolet (UV) signal at λ_{max} 269 nm (fig. S1), and HMBC correlations was proposed to be 6-amino-1-methyluracil (AmMU) bridged at C-5 with the thioether. The lack of two-dimensional (2D) NMR correlations because of the highly substituted nature of AmMU made this assignment speculative, but we were encouraged by previously reported model compounds containing thioether-bridged AmMU (fig. S1) (*15*). To ensure that we were not constrained by incorrect assumptions, MOLGEN (*16*) was used to generate all possible structures, with only AmMU fitting the spectroscopic data. Last, the products of nickel boride reduction of conazolium A were compared with synthetic AmMU (fig. S1), confirming the structure of conazolium A as shown. The calculated and measured electronic circular dichroism (ECD) spectra of conazolium A (**1**) matched relatively well (fig. S1), leading to assignment of C-2 as *S*. The structure of conazolium B (**2**) was determined similarly. Both structures were supported by tandem mass spectrometry (MS/MS) data (fig. S1). These results confirm that the colored venom glands of some cone snails are potentially rich sources of diverse, previously undescribed compounds. A complete description of structure elucidation is provided in the Supplementary Materials.

Role of *C. imperialis* small molecules in prey capture

The dominance of small molecules in *C. imperialis* distal venom glands suggested that the compounds might play a role in the hunting ecology of cones. Cone snails commonly weaponize peptide hormones, such as insulins, for hunting (*17*). Guided by this principle, we sought chemical and biosynthetic orthologs in the polychaete prey of *C. imperialis*. We expected that these might be primary, common metabolites involved in central biological processes in the polychaetes. Conazolium A (**1**) and genuanine structurally resemble ovothiol (**4**) and purines uric acid (**5**) and inosine, which are mating pheromones in polychaetes such as *Platynereis dumerilii* (*18*–*22*). Ovothiol (**4**) and uric acid (**5**) are metabolically labile, while the *C. imperialis* venom compounds do not undergo the same metabolic reactions. For example, the major inactivating reaction of ovothiol (**4**) pheromone activity is disulfide formation to give (**6**) (*18*), which is chemically impossible in **1**. We hypothesized that conazoliums and genuanine are chemical mimics of *P. dumerilii* pheromones and that they are used in an aggressive mimicry hunting strategy.

Based on an examination of stomach contents, *C. imperialis* was thought to eat amphinomid polychaetes (*23*), although little is known about its native feeding habits. However, ecological studies with these nonmodel polychaetes were difficult, as despite several tries over a period of years we could not find samples at the right stage in the mating cycle to test the hypothesis in controlled studies. Thus, a model system was required. *P. dumerilii* is one of the few polychaete model systems used in biological research (*24*), and it is consumed by worm-hunting cones (*25*, *26*). To determine whether *P. dumerilii* would provide a suitable model, we reinvestigated this question using a validated polymerase chain reaction (PCR) approach that has been recently applied to worm-hunting cones (*26*). The stomach contents of four specimens from Hawaii and the Philippines were investigated, leading to PCR products from Phyllodocida, the same order encompassing *P. dumerilii* (fig. S6). Thus, the feeding biology of *C. imperialis* is more complex than previously recorded (*24*–*26*).

We tested the aggressive mimicry hypothesis by treating the sexually mature male and female *P. dumerilii* with genuanine and conazolium A, comparing their responses with vehicle controls and with the natural external fertilization process (movies S1 to S4). A crossover study design was used in which the vehicle control was added first, followed by the test compound several minutes later (Fig. 2A). Each treatment consisted of vehicle (5% dimethyl sulfoxide or water;

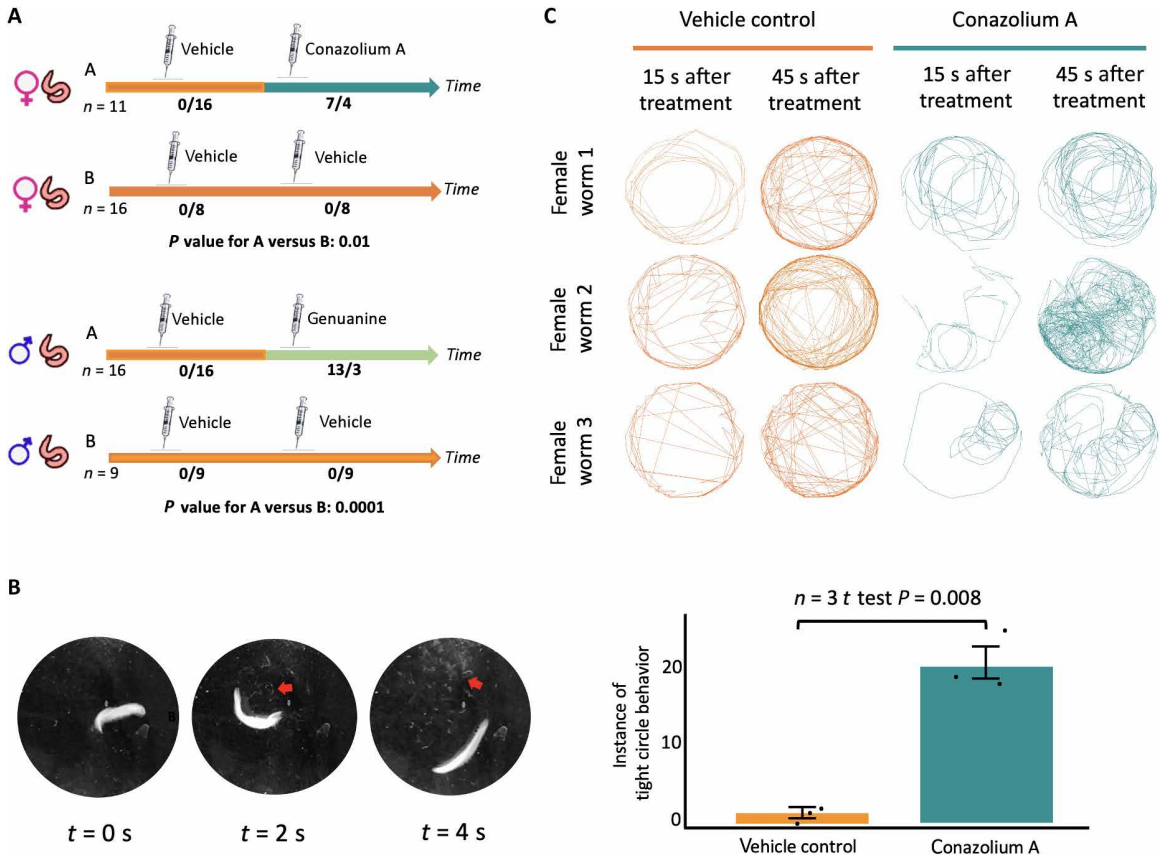

Fig. 2. Behavioral responses of sexually mature *P. dumerilii* on conazolium A and genuanine. (**A**) Schematic of experiments. Worms were treated with vehicle followed by vehicle, or vehicle followed by test compound, with positive/negative responses indicated. Fisher's exact test was applied, comparing the responses to vehicle versus responses to compound. (**B**) Genuanine induces sperm release in males. A time series of 1 worm out of the 13 positive in (A) indicates sperm release with red arrows. (**C**) Conazolium A induces female worms to swim in small tight circles, a behavior part of the nuptial dance during external fertilization. Untreated sexually mature females swim along the edges of the beaker throughout the duration of the assay. Treatment of conazolium significantly increases the tendency of female worms to swim in smaller tight circles, evident in the first 15 s. Videos of the assay and the natural mating process are found in movies S1 to S4.

25 μl), with or without 2.5 μmol of test compound, added to the worms swimming in 70-ml seawater. Biological replicates were performed by different investigators during different mating cycles (different months).

The amount of compound to be used in each assay was estimated in comparison to the isolated yield from native venom ducts. To provide further confidence that an ecologically relevant amount of compound was used in each assay, a standard curve for conazolium A was generated using high-performance liquid chromatography (HPLC), revealing that conazolium A was present at a concentration of ~150 μM considering the whole venom gland, or an astonishing 19% of the dry weight of the venom gland. A previous experiment provided a similar order of magnitude estimate for genuanine (*13*) so that overall small molecules comprise ~50% of the dry weight of the gland. Assuming that not all of the venom duct contents are expelled in a single encounter with prey, we designed experiments that used about one-fifth of that concentration.

The native pheromone uric acid causes immediate sperm release by mature males (*20*). The first biological replicate consisted of injection of vehicle followed by genuanine in seven individual male worms. While none of the worms responded to vehicle, five of seven responded to genuanine by releasing sperm. A comparison of vehicle versus genuanine response for these seven worms provided a Fisher's exact test *P* value of 0.02 (Fig. 2B). In a second biological replicate, nine worms were treated only with vehicle followed by vehicle, and nine with vehicle followed by genuanine. No worms responded to vehicle, while eight of nine released sperm clouds in response to genuanine. When the results from these 25 worms were compared, the results were significant (Fisher's exact test, $P = 0.0001$; Fig. 2), revealing that genuanine induces a pheromonal response in male *P. dumerilii*.

When females are exposed to males or to male pheromones, the worms swim in a tight circle pattern before spawning (*21*). Two tests were used. In the first, female worms ($n = 4$) were examined by filming and quantifying their swimming response upon addition of conazolium A. While the four worms did not respond to the initial treatment with vehicle, after addition of conazolium A three of them exhibited the tight-swimming response (Fig. 2C). The number of tight circles over 15 s was quantified in the responsive animals, and the difference in swimming behavior between the vehicle and conazolium A treatments was significant (*t* test, $P = 0.008$).

We performed this internal crossover-controlled experiment because the behavioral variability of female worms was high in comparison to males, making comparisons between individuals more

challenging. However, the clear results from this first experiment led us to perform a series of further experiments comparing vehicle-only worms to those treated with conazolium A. We used only worms that had a typical large-circle swimming pattern before the experiment in the analysis. Over 5 days of experiments, a total of eight females were in the vehicle control group, and seven females were treated with conazolium A. All eight of the controls did not change swimming behavior in response to treatment, while four of the seven worms treated with conazolium A exhibited the tight-swimming behavior. When all experiments with all 19 females were analyzed with a yes/no metric for tight-swimming behavior, Fisher's exact test gave a *P* value of 0.01 (Fig. 2), revealing a significant response of female worms to conazolium A treatment.

Overall, both genuanine and conazolium A initiated significant responses in polychaete worms that were very similar to responses to native worm pheromones. To determine how this experiment might reflect natural predation patterns, we recorded *C. imperialis* preying upon amphinomid polychaetes in an aquarium. *C. imperialis* was observed harpooning prey animals. In one video, *C. imperialis* was observed seeking a polychaete that had hidden inside of a small hole in the aquarium (movie S5). *C. imperialis* speared the worm and pulled it out of the hole, potentially reinforcing the idea that venom compounds are needed to entice polychaetes out of hiding places (movie S6). The colored venom can be observed injected into prey (movie S7). In some videos, as seen in a previous report (*25*), the harpoon was released, while in others the harpoon served as a tether to hold the prey.

Biosynthesis of conazolium A and ovothiol in cones and polychaetes

Conopeptides are locally produced by specialized cells lining the venom glands, where they are immediately available for prey capture (*27*). We sought to determine whether small molecules present in the gland are also locally produced. The early gene involved in ovothiol biosynthesis (*ovoA*) is conserved in animals, while later steps to ovothiol and conazoliums are convergent and/or unknown (*28*). Therefore, *C. imperialis* and other *Conus* venom gland transcriptomes were examined for the presence of *ovoA* homologs. In *C. imperialis*, both whole venom glands and ducts sectioned by color were used. An *ovoA* homolog, *conA*, was discovered in the glands of *C. imperialis* containing conazoliums, but only in the forward colored section. There, it was highly abundant, as compared to other sections of the gland closer to the venom bulb (fig. S2). To test the potential role of ConA in conazolium biosynthesis, the protein was overexpressed in *Escherichia coli*, purified it to homogeneity, and used in biochemical assays with cysteine and histidine (*29*, *30*). Efficient formation of the expected ovothiol intermediate was observed (Fig. 3 and fig. S3). These data provide evidence that, like conopeptides, conazoliums or their biochemical precursors are produced in epithelial cells of the distal venom gland.

ovoA-like biosynthetic gene transcripts were also detected in nine other species of cone snails in the collection, showing that ovothiol or its derivatives may be present in several different cones. A survey of *ovoA* homologs in polychaete worms revealed that the transcripts were present in all available databases, including amphinomid

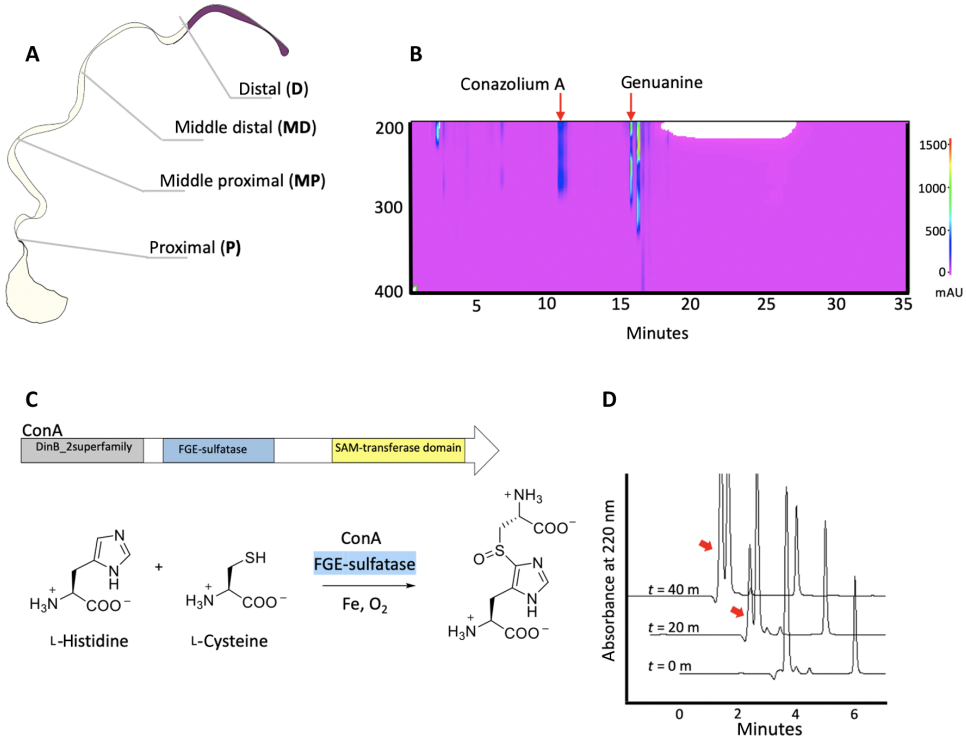

Fig. 3. ConA discovery and biochemistry. (**A**) Schematic diagram dividing the venom gland into four different sections. Small molecules are mainly found in the proximal sections of *C. imperialis*. (**B**) HPLC-diode array detector analysis of conazolium A and genuanine in the proximal section of the venom gland. (**C** and **D**) ConA catalyzes the first step of conazolium biosynthesis through the formation of histidylcysteine using histidine and cysteine [red arrows in (D)].

worms, although reassembly of the raw data was occasionally required (table S3 and fig. S2). The synthesis of ovothiol or related metabolites may be universal in polychaetes.

Chemical variation and speciation in *Stephanoconus*

An initial mystery was that we could not always isolate conazolium A from all *C. imperialis* specimens. Therefore, a metabolomics survey of *C. imperialis* specimens was performed to determine the pattern of occurrence of conazolium A and other small molecules in the snails. Notably, we found that the distal venom components of *C. imperialis* could be split into two clearly discernible branches (Fig. 4). One of these was found in *C. imperialis* specimens from relatively deeper, colder waters. We first characterized this branch from specimens collected near Cebu, Philippines, at a depth of −150 to −210 m. These deep-water specimens always contained conazoliums A and B, as well as genuanine. The other metabolic branch consisted of specimens from relatively shallower, warmer waters, first characterized from Cebu specimens collected at depths of −30 to −60 m. These specimens universally lacked conazoliums, but they instead contained neuroactive amino acids such as tryptophan and histidine, as well as neurotransmitters such as serotonin and glutamate-derived metabolites.

The deep- and shallow-water specimens were also physically different from each other: The deep-water *C. imperialis* tended to be

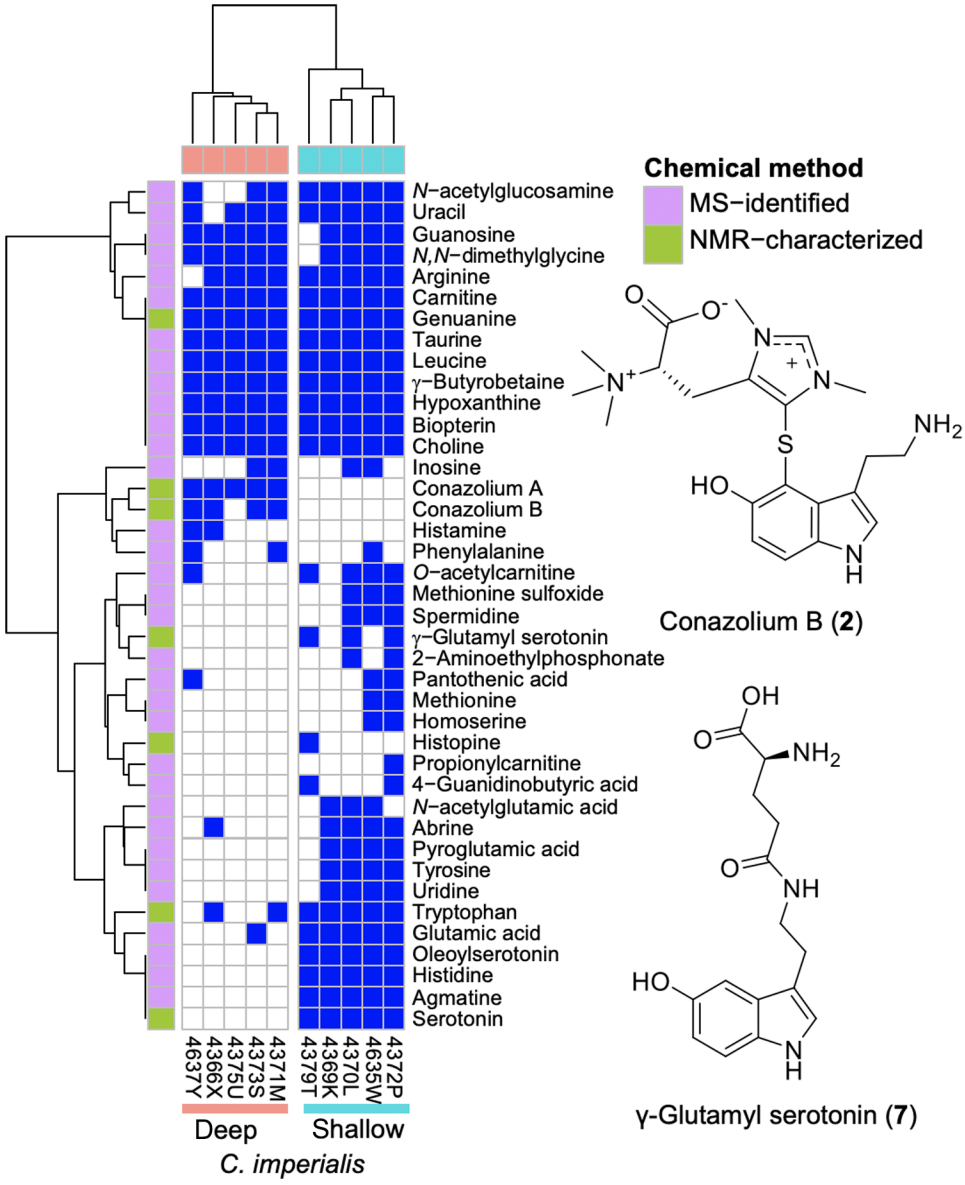

Fig. 4. Metabolomic analysis of cone snail chromatic venoms. Comparison of metabolomes from five specimens each of deep- and shallow-water *C. imperialis* from the Philippines. A blue block indicates that the compound is present in the sample (based on ultra performance liquid chromatography-HRESIMS). Compounds shown in pink were identified using the GNPS database, which analyzes molecular fragments. Compounds shown in green were compared with authentic standards that were verified using NMR experiments. Although inosine and guanosine are minor products identified in the metabolomics work, of note, they are also known as native sperm-release pheromones of polychaete worms.

smaller, have pronounced spires, free of periostacum, and with slightly different shell patterns than shallow *C. imperialis* (Fig. 5 and fig. S4). Their distal venom glands had a greenish yellow color, rather than the very dark red of the shallow specimens. These trends could be observed over a large geographical radius encompassing specimens from the Philippines, Hawaii, and Vanuatu. Thus, we hypothesized that deep- and shallow-water specimens represented genetically distinct groups of *C. imperialis*. Elements related to habitat depth might also drive different hunting strategies within a genetically homogeneous population.

To test these hypotheses, a phylogenetic tree was constructed using the mitochondrial cytochrome c oxidase I (COI) gene sequence, focusing on the *Stephanoconus* sub-genus of which *C. imperialis* is a member. *C. imperialis* deep- and shallow-water specimens diverged into two genetically distinct populations. Using the COI gene from an available specimen (table S4), we found that the chemically similar *C. genuanus* also lies within a clade that includes all of the known members of *Stephanoconus* (Fig. 5).

Potential pharmaceutical relevance in mammalian target assays

Conopeptides used in hunting have been extensively exploited as pharmaceuticals and drug leads (*10*). We sought to determine the potential of conazolium A in medicine. Conazolium A is a competitive antagonist of acetylcholine (ACh)–evoked currents mediated by human α7 nicotinic ACh receptor (nAChR) (*31*) to 100 μM ACh, with an IC_{50} (half-maximal inhibitory concentration) of 24.4 [95% confidence interval (CI), 19.9 to 35.2] (Fig. 6). This potency is consistent with what is typically found in natural red venom. Conotoxin peptides often target nAChRs, disabling prey through various mechanisms (*32*). It is thus possible that conazolium A augments the activity of peptides such as the known *C. imperialis* α7 blocker

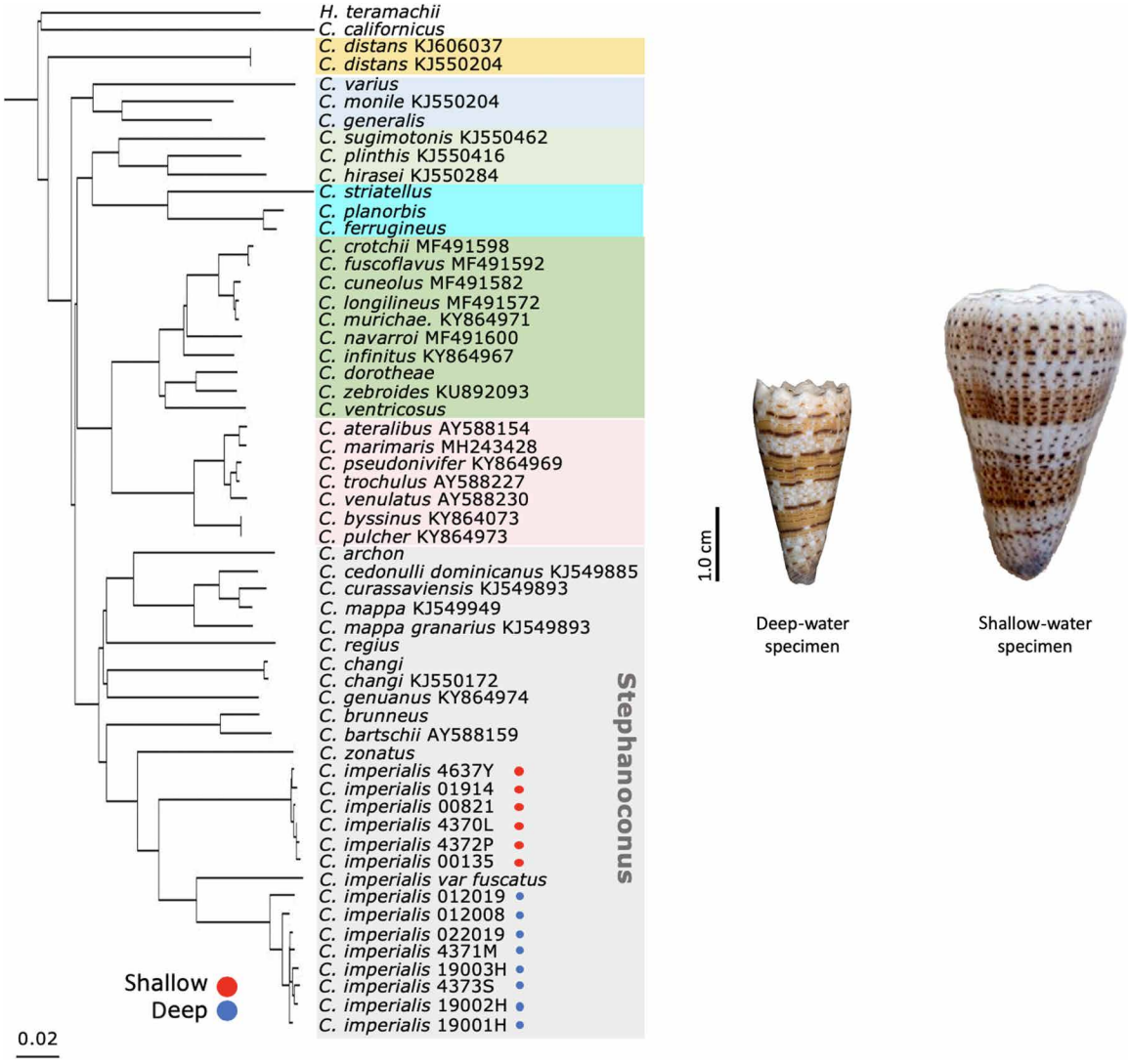

Fig. 5. Phylogeny of deep- and shallow-water *C. imperialis* variants. Left: Phylogenetic tree of *Stephanoconus* and other clades of vermivorous *Conus* species, using mitochondrial COI marker. *Profundiconus teramachii* and *Californicus californicus* are used as outgroups. COI sequences generated from this work and from others used to construct this tree are listed in table S4. Right: Deep- and shallow-water specimens of *C. imperialis*.

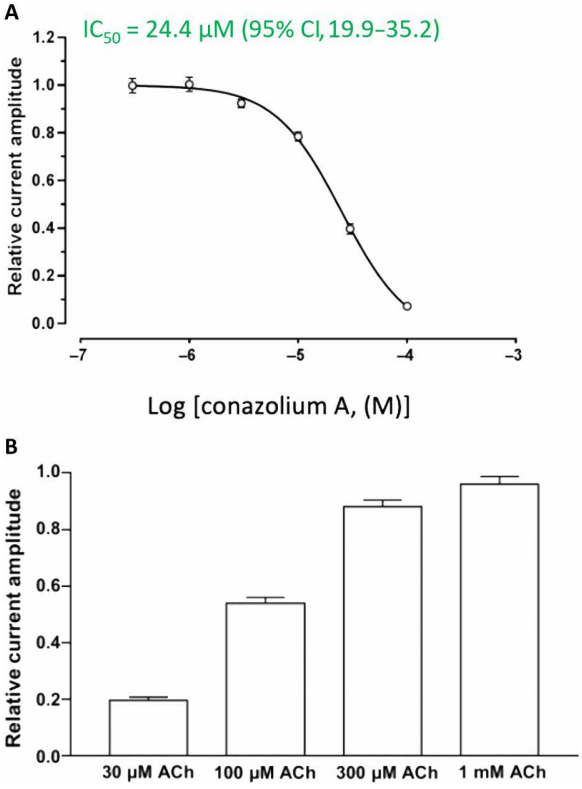

Fig. 6. Activity of conazolium A in human α7 nAChR. (**A**) Concentration-response relationship of relative ACh-evoked current amplitude mediated by human α7 nAChR in the presence of conazolium A ($n = 5$). (**B**) Concentration response of relative ACh-evoked current amplitude mediated by human α7 nAChR in the presence of 25 μM conazolium A ($n = 6$ to 7).

conotoxin ImI (*12*). γ-Glutamyl serotonin and L-tryptophan showed modest activity in mouse dorsal root ganglion (DRG) neurons (*33*), activating a small population of neurons (table S5).

DISCUSSION

Here, we show that what was previously described as a single species, *C. imperialis*, is likely composed of two different species. The deep- and shallow-water clades of *C. imperialis* are more genetically distant from each other than they are from *C. imperialis* cf. *fuscatus*, which many researchers consider to be the distinct species, *Conus* (or *Rhombiconus*) *fuscatus* (*34*). Deep- and shallow-water *C. imperialis* also occupy the same geographical range across the oceans, yet retain their genetic distinctiveness. Overall, the data suggest taxonomic reinvestigation of this species and its close relatives.

Each of these potentially different species uses a consistent mixture of bioactive small molecules, synthesized in the distal venom gland, for prey capture. The shallow-water *C. imperialis* contains abundant amounts of neurotransmitters such as serotonin and glutamate, as well as related compounds, which are likely involved in predation based on previous studies. For example, serotonin activates or retards swimming in polychaetes and other annelids (*35*). Glutamate has been identified as a part of a polychaete mating pheromone cocktail (*21*), while γ-glutamyl serotonin is a known annelid metabolite (*36*). Histopine is similar to fish attractant compounds (*37*), and oleoyl-serotonin is a low-micromolar transient receptor potential cation channel subfamily V (TRPV1) antagonist (which would potentially block pain signals) (*38*). By contrast, deep-water *C. imperialis* contains conazoliums A and B. Both shallow- and deep-water *C. imperialis*, as well as the related *Stephanoconus* species *C. genuanus*, contain genuanine. Thus, as is found in cone snail peptide venoms, the small molecule venom components constitute a complex cocktail, which might be repurposed for targeting prey in different habitats.

In this study, we show that conazolium A and genuanine, like serotonin, exhibit profound physiological effects on polychaetes, and therefore, we propose that these novel compounds are also important for successful hunting. The compounds resemble native polychaete pheromones, which include ovothiol, urate, guanosine, and inosine in various worm species (*18*–*21*). When added to sexually mature *P. dumerilii*, conazolium A and genuanine induce mating behaviors that are similar to those induced by the natural pheromones, including sperm release and mating dance (*39*). Conazolium A and genuanine may serve either as attractants or as neuromodulators in worm prey.

The use of pheromone mimics has been described before in the chemical aggressive mimicry strategy used by *Mastophora* sp. spiders, although not previously in venoms (*40*–*42*). In aggressive mimicry, a predator imitates the native attractants of prey animals to lure them in for the kill (*43*, *44*). *Mastophora* spiders secrete a chemical lure: The spiders coopt the pheromones that their prey natively use as sexual attractants. What is different here is that, unlike *Mastophora*, *C. imperialis* does not make the same pheromones found in prey polychaetes. Instead, it makes more chemically stable mimics of those pheromones. Such a strategy is important because, like the stable analogs of hormones used in human birth control pills (*45*), the resulting compounds work independently of the prey's metabolism, potentially overwhelming the normal mating systems.

Furthermore, polychaetes often remain hidden within tubes or crevices, and thus, it is tempting to speculate that conazolium and genuanine might be used to draw them out of otherwise hidden and inaccessible burrows. This idea is analogous to the King's Gambit, a classical chess move in which the king uses two pawns to draw out the opponent. *C. imperialis*, the imperial cone (named after the "crown" atop its shell), might use its two pawns conazolium and genuanine in an analogous manner.

The current study, while opening up a new area of venom research, has several limitations. First, the real-world situation is much more complicated than can be recapitulated in laboratory assays. Worm-hunting cones target many different polychaete species, and although there is some indication that polychaete pheromones are highly promiscuous in their cross-species activity (*46*, *47*), limited information is available given the >8000 polychaete species. The venom toxin mixtures contain many more bioactive compounds, such as conopeptides, which would add to the complexity of the response in nature. This mimics the known complexity of native pheromones, which also comprise much more complex mixtures than simply ovothiol and uric acid. The hunting strategies of vermivorous cone snails in nature are also almost completely unknown and remain unaddressed in this work. In short, although genuanine and conazolium mimic polychaete pheromones, how the compounds fit into the overall worm-hunting strategy requires more research. The present study suggests a path forward for future field research of cone-hunting strategies.

In a second limitation, while we provide genetic and biochemical evidence that functional ovothiol genes are abundantly expressed in

the *C. imperialis* venom gland, we have not yet identified late-stage enzymes that would be involved in specialization of ovothiol into the conazolium natural products. Further work is ongoing to uncover these and other biosynthetic genes.

Cone snails have long been studied for their potential medical applications, leading to an approved drug and many compounds in clinical trials. So far, all of these drugs are peptides, which are not orally bioavailable and must be injected. Here, we show that small molecules are also active components of some venoms with pharmaceutical potential. Small molecules have some advantages in that they are often orally bioavailable, making it possible to take them in pill form (*48*). Conazolium A was active on targets in polychaetes, as well as a nAChR antagonist. While the compound was modestly acting on the human receptor, it is a new lead scaffold for the design of small molecules targeting nAChRs.

Here, we discovered a biological interaction in which venom component small molecules mimic native prey pheromones in a twist on aggressive mimicry. In this process, primary metabolic biosynthesis involved in central metabolism is repurposed for prey capture through simple modifications to the primary metabolites, ovothiol and guanosine. It seems likely that, given the many venomous animal species, a biology-first approach to natural products discovery should yield many more unexpected roles for chemistry in nature.

MATERIALS AND METHODS

Sample collection

Cone snails were collected either by SCUBA or by using gill nets. Geographic location and period of cone snail collection used in this work are listed in table S1. Snails were dissected, and venom glands were divided into four sections (distal, middle distal, middle proximal, and proximal). Sectioned tissues are stored in RNAlater and flash-frozen in liquid nitrogen before total RNA extraction and chemical analysis (Supplementary Materials).

Identification of small-molecule components in venom

Crude venom extracts were prepared from proximal sections by extraction with 200 to 1000 µl of H_2O. The volume used for extraction varied according to tissue size. Briefly, proximal tissue sections in 1.5-ml microcentrifuge tubes were mixed with nanopure water and vortexed for 5 min. The mixture was centrifuged at 3739*g* for 10 min at 4°C to recover the crude venom extract.

Conazoliums A and B were purified from crude venom extracts of deep water species of *C. imperialis* using HPLC with a gradient from 5 to 100% MeCN in water containing 0.05% trifluoroacetic acid (TFA) over 40 min to yield conazolium A (**1**) (1.0 mg, retention time (rt) = 7.1 min; 0.3 mg per venom gland), conazolium B (**2**) (2.3 mg, rt = 6.6 min; 0.8 mg per venom gland), and genuanine (0.6 mg, rt = 7.8 min; 0.2 mg per venom gland). Structures were elucidated using 1D and 2D NMR spectroscopy (see the "Structure elucidation of conazoliums" section in the Supplementary Materials). ECD calculation was performed as previously described (*49*). Possible structures for the AmMU part of conazolium A were generated using MOLGEN (*16*), with the following input formula: "C[sp3,h=3,d=0]1C[sp2_a,h=0]4H7N[val=3]3S[val=2,d=0,h=1]O2." All 182 output structures were manually examined and compared to the spectroscopic data.

To reduce conazolium A for confirmation of the aminouracil moiety, conazolium A (50 µg) was dissolved in MeOH/THF/H_2O (300 µl; 1:2:1), and $NiCl_2$ (1.0 mg, 0.008 mmol) was added to the solution. After stirring for 1 min, $NaBH_4$ (1.0 mg, 0.026 mmol) was added, and stirring was continued for 1 hour. The mixture was centrifuged, and the supernatant was directly used for C18 HPLC analysis with a gradient from 5 to 100% MeCN in water containing 0.05% TFA over 40 min.

Conazolium A (**1**): pale yellow solid; UV (MeOH) λ_{max} 224, 269 nm; ECD (0.5 mg/ml, methanol), λ_{max} ($\Delta\varepsilon$) 269 (1.5) nm; ^1H and ^{13}C NMR (table S2); high resolution electrospray ionization mass spectrometry (HRESIMS) *m/z* 397.1643 $[M]^+$ (calcd for $C_{16}H_{25}N_6O_4S^+$, 325.1653).

Conazolium B (**2**): pale yellow solid; UV (MeOH) λ_{max} 235, 297 nm; ECD (0.5 mg/ml, methanol), λ_{max} ($\Delta\varepsilon$) 240 (−1.2), 256 (0.7), 287 (0.6), 327 (−0.5) nm; ^1H and ^{13}C NMR (table S2); HRESIMS *m/z* 432.2062 $[M]^+$ (calcd for $C_{16}H_{25}N_6O_4S^+$, 432.2064).

The venom extract of shallow-water specimens of *C. imperialis* was purified using the same HPLC gradient as for the deep water specimens, with an Agilent Eclipse XDB-C18 column (10 × 250 mm, 5 µm), to yield histopine (3.0 mg, rt = 2.4 min; 0.7 mg per venom gland), genuanine (0.5 mg, rt = 3.9 min; 0.1 mg per venom gland), γ-glutamyl serotonin (0.8 mg, rt = 12.4 min; 0.2 mg per venom gland), and tyrosine (0.1 mg, rt = 14.6 min; 0.02 mg per venom gland).

To determine the yield of **1**, a standard curve was constructed by injecting each dilution of pure conazolium A (8.0, 4.0, 2.0, 1.0, and 0.5 mg/ml in 5 µl of MeOH) into a Kinetex 5 µm HILIC 100A LC Column 250 × 4.6 mm; HPLC mobile phase: 76% MeCN in water with 0.005% TFA; flow rate: 1 ml/min; peak detection: 268 nm. A piece of venom duct (~1 cm) was cut and weighed (2.8 mg) on an analytical balance. The venom duct was lyophilized (dry weight, 0.9 mg) and extracted with 1:1 water:MeCN (400 µl). The extract (20 µl) was injected onto the same HPLC column, and the yield of **1** was calculated as 174 µg (150 µM in wet venom duct tissue; 19% of dry weight).

Metabolomics analysis

The MS/MS spectra of the 11 cone snail red venom gland extracts were generated using Agilent 6530 Q-TOF LC/MS with a Kinetex HILIC column (2.6 µ, 100 A, 100 × 4.6 mm, 1 ml/min) with a gradient from 100 to 50% MeCN in 20 min. The raw LC-MS/MS data were converted to mgf format using MassHunter. The mgf version of the data was used to generate a molecular network using the Global Natural Products Social Molecular Networking web site (*50*), with standard parameter and MSCluster option turned off. The output result was visualized using Cytoscape 3.7 software (*51*).

Behavioral assays

P. dumerilii behavioral assay was performed using a modified version of a previously reported protocol (*18*). Sets of worms from different mating cycles (February, August, and September 2020) were used in the experiment. Sexually mature *P. dumerilii* were sex-typed and individually placed in 100-ml glass beakers containing about 70-ml filtered seawater at room temperature (19° to 20°C). Worms were allowed to acclimatize for 15 min. The test compounds and vehicle controls were tested on the same specimen. Vehicle control was applied first followed by a rest period of 5 min before application of test compounds. Conazolium A and genuanine were added by injecting 25 µl (100 mM) near the female and male worms' periphery, providing a concentration of ~35 µM. A positive response was recorded when male worms released sperm cloud upon exposure to genuanine and when female worms swam in tight small circles. All assays were video-recorded (examples provided in movies S1 to S4),

and responses to conazolium A were processed using a custom-built tracking software. A total of 25 male and 19 female worms were used in these assays, over 3 months. Biological replicates were conducted during different maturation cycles (different months).

Videos of female behavior were analyzed using a custom-built pipeline, Ruby-Tracker (https://github.com/pflorez/Ruby-Tracker), which allowed quantification of swimming behavior. In brief, all videos were transformed into an 8-bit format. An average video frame was computed for each video and then used to subtract the background of each frame. A circular binary mask was manually selected using the average video frame to limit the region of interest for the inside of the glass beaker and thus avoid possible reflections on the beakers wall to affect the tracking result. A global threshold was manually implemented. The binarized videos were then used to track the position of the free-swimming worm in every frame. Post hoc analysis and trace map generations were done using R version 3.6.3.

Statistical analyses

Mean ± SE was calculated using R package (ggpubr) and plotted using ggbarplot function. The *P* values between gene expression levels were calculated using T.test method using stat_compare_means function. Fisher's exact test was calculated using fisher.test() function in R 3.5.2 package. nAChR assays used mean ± SEM calculated with GraphPad Prism 7.

Transcriptome sequencing and analysis

RNA was extracted from venom glands using the Direct-zol RNA extraction kit (Zymo Research, Irvine, CA, USA) following the manufacturer's protocol. In one case, a *C. imperialis* venom gland was manually sectioned before processing, while in others the colored part of the venom gland was used. Extracted RNA was submitted to the Huntsman Cancer Institute's High Throughput Genomics Core Facility, where complementary DNA (cDNA) library preparation and sequencing was performed. Transcriptomes of *C. imperialis* red venom gland were sequenced using an Illumina HiSeq 2000 sequencer with ~350–base pair (bp) inserts and 125-bp paired-end runs. Computation was performed at the Center for High Performance Computing at the University of Utah. Raw reads were trimmed by Trimmomatic-0.39 (parameters PE -phred33 ILLUMINACLIP: TruSeq3-PE-2.fa:2:30:10 LEADING:3 TRAILING:3 SLIDINGWINDOW:4:15 MINLEN:50). Trimmed reads for each specimen were de novo assembled using rnaSPAdes (*52*) with default parameters.

Protein-coding genes for each assembly were predicted using Prodigal 2.6.3 (*53*). The duplicated genes across specimens were removed according to blastn comparison result (identity = 100%). The remaining protein-coding genes from each assembly were combined as a reference genome. The trimmed raw reads of each specimen were multi-mapped to the reference genome assembly using bowtie 1.2.3 (*54*) (--all -S index). The multitude of contigs produced by assembly was hierarchically clustered, and cluster count summarization was performed using Corset 1.04 (*55*) according to shared read information. Transcript abundance of genes was estimated using EdgeR (*56*) by normalized counts per million. *COI*, *conA*, and reference genes from each specimen were manually obtained using blastn.

Determination of gut contents of *C. imperialis*

Four different *C. imperialis* specimens were dissected, and the DNA was extracted. Nested PCR was used to identify polychaete 16*S* ribosomal RNA (rRNA) gene content in the cone snail gut metagenome. OneTaq 2X Master Mix with Standard Buffer was used with the following conditions: 95°C for 5 min followed by 40 cycles of [90°C for 10 s, 54°C for 30 s, 68°C for 20 s]. First, primers 16S_general_worm_F: CAGAGGCTACATACC and 16S_general_worm_R: CTAAGCCAACATCGAGG were used. For nesting, the second round used primers 16S_internal_Pdumerilli_F: CCAGCCTGTTTATCAAAAACAC and 16S_internal_Pdumerilli_R: GTCTTTTGGTTGTCCCAAC. The PCR products with the anticipated size were gel-purified, cloned, and sequenced. The resulting sequences were analyzed by aligning them with rRNA gene sequences of marine annelids (order Phyllodocida) available in GenBank, using Geneious Alignment (global alignment with free end gaps). A phylogenetic tree was constructed using the unweighted pair group method with the Jukes-Cantor model, using 100 bootstrap replicates. The tree and alignments were made using the Geneious Prime 2020.2.3 software package.

Cloning and expression of *conA* gene in *E. coli*

conA was amplified by PCR using products of first-strand cDNA synthesis of venom gland total RNA as template. First-strand DNA synthesis was performed using SuperScript III First-Strand Synthesis System (Thermo Fisher Scientific. USA). *conA* was cloned into pET-21b(+) by restriction cloning. Amplified *conA* was digested with Nde I and Bam HI (New England Biolabs) and was ligated into a linearized pET-21b(+) backbone to yield plasmid pJPTConA, which was sequenced before expression in *Escherichia coli* BL21(DE3) (New England Biolabs). A single *E. coli* colony was picked and cultured overnight in LB broth media (50 ml) supplemented with kanamycin (50 μg/ml) at 30°C at 200 rpm. For protein expression, the overnight culture (10 ml/liter) was then inoculated into LB (4 × 1 liter) supplemented with kanamycin (50 μg/ml) and incubated at 30°C at 200 rpm until OD_{600} (optical density at 600 nm) = 0.6. The cultures were cooled down to ~15°C before addition of 1 M isopropyl-β-D-thiogalactopyranoside (IPTG) (50 μl). Expression of soluble ConA as the C-terminally His-tagged construct by IPTG induction was carried out by incubating the cultures in 15°C at 200 rpm for 16 hours. Cell pellets were harvested by centrifugation at 3739*g* for 20 min at 4°C after induction. Pellet was resuspended in lysis buffer [50 mM tris-HCl, 150 mM NaCl, 10 mM imidazole, 10% glycerol, lysozyme (600 μg/ml), pH 7.5]. The suspension was incubated at 4°C before for 30 min before sonicating thrice with 30-s intervals. Deoxyribonuclease (20 μg/ml) was added, and the lysate was further incubated for further 15 min until the homogenate was no longer viscous. The homogeneous mixture was centrifuged at 28,928*g* for 40 min at 4°C to separate the supernatant from cell debris. The supernatant was filtered with a 0.45-μm polyvinylidene difluoride syringe filter (Millex-HV, Sigma-Aldrich) before adding Ni–nitriliotriacetic acid and incubating the mixture at 4°C for 30 min. Soluble ConA was recovered from the resin by washing the resin twice with 10-ml wash buffer (50 mM tris-HCl, 1 M NaCl, 10 mM imidazole, pH 8.0) followed by a series of elution buffers (1 M NaCl, imidazole at pH 8.0) with increasing concentration of imidazole (50, 100, 200 mM imidazole). The protein-containing fraction was desalted and concentrated using Amicon Ultra 30 MWCO centrifugal filters (EMD Millipore) by centrifugation at 3739*g* for 20 min at 4°C.

In vitro characterization of ConA

Enzyme reaction mixtures (100 μl) consisted of enzyme ConA (2 μM), 50 mM tris-HCl (pH 8.0), 20 mM NaCl, 1 mM histidine, 1 mM tris(2-carboxyethyl)phosphine, 0.1 mM $FeSO_4$, and 1 mM sulfur-donor substrates (cysteine, glutathione, methionine, and *N*-acetyl cysteine).

The reaction mixture was incubated at room temperature for 20 min and quenched by addition of 30 μl of water with 1.0% TFA. An aliquot (20 μl) of the reaction mixture was diluted in 70 μl of H_2O and analyzed by HPLC. HPLC analysis was performed using a Hitachi Primade HPLC system equipped with a DAD detector and autoinjector. Aliquots (20 μl) of the sample were injected onto a reversed-phase C18 analytical column (Luna C18 4.6 × 100 mm, Phenomenex) with a gradient starting at 0% mobile phase B (H_2O + 0.1% TFA: MeCN) for 5 min and increased until 5% mobile phase B for 20 min at a rate of 0.7 ml/min. The reaction product was purified by HPLC and characterized by NMR (fig. S3C).

COI analysis

Genomic DNA was extracted from foot or body tissue using the Gentra PUREGENE DNA Isolation Kit (Gentra Systems, Minneapolis, MN) according to the manufacturer's standard protocol. Genomic DNA (10 ng) was used as a template for PCR with oligonucleotides corresponding to LCOI-1490 (5′-GGTCAACAAATCATAAAGAY-ATGYG) and HCOI-2198 (5′-TAAACTTCAGGGTGACCAAARAAYCA) COI gene segments (*57*). PCR was performed with Advantage 2 Polymerase Mix (Clontech Laboratories Inc., CA, USA) using the following method: initial denaturation (95°C, 60 s), followed by 40 cycles of denaturation (95°C, 20 s), annealing (55°C, 20 s), and extension (72°C, 30 s).

The resulting PCR products were purified using the PureLink PCR Product Purification Kit (Invitrogen Life Technologies, Carlsbad, CA) following the manufacturer's suggested protocol. The eluted DNA fragments were annealed to pNEB206A vector, and the resulting products were transformed into competent DH5a cells, using the USER Friendly Cloning Kit (New England BioLabs Inc., Beverly, MA) following the manufacturer's protocol. The nucleic acid sequences from six each of these COI-encoding clones were determined by automated sequencing (Core Sequencing Facility, University of Utah, USA) and deposited into GenBank. Phylogenetic analysis was performed using the COI barcode sequence for each species. The sequences were aligned, and neighbor-joining trees were generated using ClustalX with standard default options (*58*). The tree was visualized using Tree Dyn 198.3 (*59*).

DRG assay (*60*)

Lumbar DRG cells were harvested from calcitonin gene-related peptide-green fluorescent protein (CGRP-GFP) mice (in a CD1 genetic background), postnatal 25 (P25) to P56 days old, and plated in 24-well plates in Dulbecco's modified Eagle's medium, supplemented with 10% (v/v) fetal bovine serum (FBS), penicillin (100 U/ml), streptomycin (100 μg/ml), 1× Glutamax (Invitrogen), 10 mM Hepes, and 0.4% (w/v) glucose, with final pH adjusted to 7.4. After overnight incubation, cells were loaded with 2.5 μM fluorescent ratiometric calcium probe Fura-2-AM for 1 hour at 37°C, followed by equilibration at room temperature for 30 min. DRG cells were incubated with the compounds for 6 min in between 20 mM KCl pulses (15-s application). To identify the subtype of neurons, cells were pulsed with various compounds as described (*61*). Fluorescence emission at 510 nm was recorded at 340- and 380-nm excitation wavelengths every 2 s. The ratio of fluorescence intensities at 340 and 380 nm was plotted over time. Approximately 700 to 1000 neurons or regions of interest were analyzed per well.

nAChR assays

In vitro synthesized (mMessage mMachine, AMBION, Foster City, CA, USA) capped RNA (cRNA) encoding human α7 nAChR was injected into stage V to VI *Xenopus laevis* oocytes. Oocytes were incubated at 18°C in sterile ND96 solution composed of 96 mM NaCl, 2 mM KCl, 1 mM $CaCl_2$, 1 mM $MgCl_2$, and 5 mM Hepes at pH 7.4, supplemented with 5% FBS, gentamicin (0.5 mg/liter) (GIBCO, Grand Island, NY, USA), and penicillin-streptomycin (100 U/ml; GIBCO, Grand Island, NY, USA). Electrophysiological recordings were carried out 2 to 7 days after cRNA microinjection. Two-electrode voltage clamp recording of *X. laevis* oocytes expressing nAChRs was carried out 2 to 7 days after cRNA microinjection at room temperature (21° to 24°C) using a GeneClamp 500B amplifier and pClamp9 software interface (Molecular Devices, Sunnyvale, CA, USA) at a holding potential of −80 mV. Oocytes were briefly washed with ND96 (bath solution) at a rate of 2 ml/min followed by three applications of half-maximal effective concentration (EC_{50}) ACh of 100 μM. Washout with bath solution was done for 3 min between ACh applications. Oocytes were incubated with different concentrations of conazolium for 5 min, with the perfusion system turned off, followed by co-application of ACh. Conazolium competitive antagonism at human α7 nAChR was performed by applying increased concentration of ACh (30 μM to 1 mM) in the presence of conazolium at IC_{50} of 25 μM. All modulator solutions were prepared in ND96 + 0.1% bovine serum albumin. Peak current amplitudes before (ACh alone) and after (ACh + conazolium) conazolium incubation were measured using Clampfit 10.7 (Molecular Devices, Sunnyvale, CA, USA), where the ratio of ACh + conazolium–evoked current amplitude to ACh alone–evoked current amplitude was used to assess modulatory activity. Recordings at each concentration were pooled (n = 4 to 6) and represent means ± SEM. The concentration-response relationship for conazolium was analyzed using the Hill equation and IC_{50} reported with 95% CI (Prism 7, GraphPad Software, La Jolla, CA, USA).

Patch clamp ion channel assays

Patch clamp recordings were made at room temperature (20° to 22°C) with the MultiClamp 700B Amplifier, digitalized with Digidata 1440, and controlled with pClamp11 software (Molecular Devices, USA). Whole-cell currents were sampled at 100 kHz and filtered to 10 kHz, with series resistance compensated 60 to 80%. Fire-polished borosilicate (2 to 4 megohms) (1B150F-4, World Precision Instruments, USA) patch pipettes were filled with intracellular solutions containing 140 mM K-gluconate, 10 mM NaCl, 2 mM $MgCl_2$, 5 mM EGTA, and 10 mM Hepes (pH 7.2). Recombinant [hNav1.7, hNav1.7 + hβ1, and hNav1.8 in human embryonic kidney (HEK) 293 cells] and native voltage-gated sodium currents (I_{Na}) from mouse DRG (mDRG) neurons were recorded in extracellular solution containing 110 mM NaCl, 2 mM $CaCl_2$, 2 mM $MgCl_2$, 30 mM TEA-Cl, 10 mM D-glucose, and 10 mM Hepes (pH 7.4). After I_{Na} was recorded, the extracellular solution was exchanged to 135 mM NaCl, 2 mM $CaCl_2$, 2 mM $MgCl_2$, 5 mM KCl, 10 mM D-glucose, 10 mM Hepes (pH 7.4) to enable recording of the mDRG outward voltage-activated potassium currents (I_K). Genuanine and conazolium A (10 μM) were superfused using a syringe pump (New Era Pump Systems Inc., USA) loaded with 1-ml syringe connected to 50-cm MicroFil 28G (World Precision Instruments) at 2 μl × min^{-1}.

Animal use

All procedures were approved by the University of Utah Institutional Animal Care and Use Committee or by the University of Wollongong and University of Sydney Animal Ethics Committees.

SUPPLEMENTARY MATERIALS

Supplementary material for this article is available at http://advances.sciencemag.org/cgi/content/full/7/11/eabf2704/DC1

REFERENCES AND NOTES

1. N. Puillandre, P. Bouchet, T. F. Duda Jr., S. Kauferstein, A. J. Kohn, B. M. Olivera, M. Watkins, C. Meyer, Molecular phylogeny and evolution of the cone snails (Gastropoda, Conoidea). *Mol. Phylogenet. Evol.* **78**, 290–303 (2014).
2. B. Gao, C. Peng, J. Yang, Y. Yi, J. Zhang, Q. Shi, Cone snails: A big store of conotoxins for novel drug discovery. *Toxins* **9**, 397 (2017).
3. S. W. A. Himaya, R. J. Lewis, Venomics-accelerated cone snail venom peptide discovery. *Int. J. Mol. Sci.* **19**, 788 (2018).
4. J. W.-H. Li, J. C. Vederas, Drug discovery and natural products: End of an era or an endless frontier? *Science* **325**, 161–165 (2009).
5. B. M. Olivera, J. Seger, M. P. Horvath, A. E. Fedosov, Prey-capture strategies of fish-hunting cone snails: Behavior, neurobiology and evolution. *Brain Behav. Evol.* **86**, 58–74 (2015).
6. H. Safavi-Hemami, J. Gajewiak, S. Karanth, S. D. Robinson, B. Ueberheide, A. D. Douglass, A. Schlegel, J. S. Imperial, M. Watkins, P. K. Bandyopadhyay, M. Yandell, Q. Li, A. W. Purcell, R. S. Norton, L. Ellgaard, B. M. Olivera, Specialized insulin is used for chemical warfare by fish-hunting cone snails. *Proc. Natl. Acad. Sci. U.S.A.* **112**, 1743–1748 (2015).
7. P. Ahorukomeye, M. M. Disotuar, J. Gajewiak, S. Karanth, M. Watkins, S. D. Robinson, P. Flórez Salcedo, N. A. Smith, B. J. Smith, A. Schlegel, B. E. Forbes, B. Olivera, D. Hung-Chieh Chou, H. Safavi-Hemami, Fish-hunting cone snail venoms are a rich source of minimized ligands of the vertebrate insulin receptor. *eLife* **8**, e41574 (2019).
8. H. Safavi-Hemami, A. Lu, Q. Li, A. E. Fedosov, J. Biggs, P. Showers Corneli, J. Seger, M. Yandell, B. M. Olivera, Venom insulins of cone snails diversify rapidly and track prey taxa. *Mol. Biol. Evol.* **33**, 2924–2934 (2016).
9. J. G. Menting, J. Gajewiak, C. A. MacRaild, D. H.-C. Chou, M. M. Disotuar, N. A. Smith, C. Miller, J. Erchegyi, J. E. Rivier, B. M. Olivera, B. E. Forbes, B. J. Smith, R. S. Norton, H. Safavi-Hemami, M. C. Lawrence, A minimized human insulin-receptor-binding motif revealed in a *Conus geographus* venom insulin. *Nat. Struct. Mol. Biol.* **23**, 916–920 (2016).
10. B. M. Olivera, S. Raghuraman, E. W. Schmidt, H. Safavi-Hemami, Linking neuroethology to the chemical biology of natural products: Interactions between cone snails and their fish prey, a case study. *J. Comp. Physiol. A* **203**, 717–735 (2017).
11. J. W. Aman, J. S. Imperial, B. Ueberheide, M.-M. Zhang, M. Aguilar, D. Taylor, M. Watkins, D. Yoshikami, P. Showers-Corneli, H. Safavi-Hemami, J. Biggs, R. W. Teichert, B. M. Olivera, Insights into the origins of fish hunting in venomous cone snails from studies of *Conus tessulatus*. *Proc. Natl. Acad. Sci. U.S.A.* **112**, 5087–5092 (2015).
12. J. M. McIntosh, D. Yoshikami, E. Mahe, D. B. Nielsen, J. E. Rivier, W. R. Gray, B. M. Olivera, A nicotinic acetylcholine receptor ligand of unique specificity, alpha-conotoxin ImI. *J. Biol. Chem.* **269**, 16733–16739 (1994).
13. J. L. B. Neves, Z. Lin, J. S. Imperial, A. Antunes, V. Vasconcelos, B. M. Olivera, E. W. Schmidt, Small molecules in the cone snail arsenal. *Org. Lett.* **17**, 4933–4935 (2015).
14. J. M. McIntosh, T. A. Foderaro, W. Li, C. M. Ireland, B. M. Olivera, Presence of serotonin in the venom of *Conus imperialis*. *Toxicon* **31**, 1561–1566 (1993).
15. G. Khalili, A new synthesis of *S*-aryl uracils from aryl thiols and 6-amino uracils in the presence of NCS. *Mol. Divers.* **20**, 963–968 (2016).
16. R. Gugisch, A. Kerber, A. Kohnert, R. Laue, M. Meringer, C. Rücker, A. Wassermann, MOLGEN 5.0, A molecular structure generator, in *Advances in Mathematical Chemistry and Applications*: *Volume 1*, S.C. Basak, G. Restrepo, Jose Villaveces, Eds. (Elsevier, 2016), pp. 113–138.
17. S. D. Robinson, Q. Li, P. K. Bandyopadhyay, J. Gajewiak, M. Yandell, A. T. Papenfuss, A. W. Purcell, R. S. Norton, H. Safavi-Hemami, Hormone-like peptides in the venoms of marine cone snails. *Gen. Comp. Endocrinol.* **244**, 11–18 (2017).
18. I. Röhl, B. Schneider, B. Schmidt, E. Zeeck, L-Ovothiol A: The egg release pheromone of the marine polychaete *Platynereis dumerilli*: Annelida: Polychaete. *Zeischrift Naturforsch. C* **54**, 1145–1147 (1999).
19. E. Zeeck, T. Harder, M. Beckmann, C. T. Müller, Marine gamete-release pheomones. *Nature* **382**, 214 (1996).
20. E. Zeeck, T. Harder, M. Beckmann, Uric acid: The sperm release pheromone of the marine polchaete *Platynereis dumerilli*. *J. Chem. Ecol.* **24**, 13–22 (1998).
21. E. Zeeck, T. Harder, M. Beckmann, Inosine, L-glutamic acid and L-glutamine as components of a sex pheromone complex of the marine polychaete *Nereis succinea* (Annelida: Polychaeta). *Chemoecology* **8**, 77–84 (1998).
22. G. J. Watson, F. M. Langford, S. M. Gaudron, M. G. Bentley, Factors influencing spawning and pairing in the scale worm *Harmothoe imbricata* (Annelida: Polychaeta). *Biol. Bull.* **199**, 50–58 (2000).
23. A. J. Kohn, The ecology of *Conus* in Hawaii. *Ecol. Monogr.* **29**, 47–90 (1959).
24. E. Kuehn, A. W. Stockinger, J. Girard, F. Raible, B. D. Özpolat, A scalable culturing system for the marine annelid *Platynereis dumerilii*. *PLOS ONE* **14**, e0226156 (2019).
25. A. J. Kohn, C. Hunter, The feeding process in *Conus imperialis*. *Veliger* **44**, 232–234 (2001).
26. D. A. Weese, T. F. Duda Jr., Effects of predator-prey interactions on predator traits: Differentiation of diets and venoms of a marine snail. *Toxins* **11**, 299 (2019).
27. G. Bulaj, B. M. Olivera, Folding of conotoxins: Formation of the native disulfide bridges during chemical synthesis and biosynthesis of *Conus* peptides. *Antioxid. Redox Signal.* **10**, 141–156 (2008).
28. M. Gerdol, M. Sollitto, A. Pallavicini, I. Castellano, The complex evolutionary history of sulfoxide synthase in ovothiol biosynthesis. *Proc. Biol. Sci.* **286**, 20191812 (2019).
29. A. Braunshausen, F. P. Seebeck, Identification and characterization of the first ovothiol biosynthetic enzyme. *J. Am. Chem. Soc.* **133**, 1757–1759 (2011).
30. N. Naowarojna, P. Huang, Y. Cai, H. Song, L. Wu, R. Cheng, Y. Li, S. Wang, H. Lyu, L. Zhang, J. Zhou, P. Liu, *In vitro* reconstitution of the remaining steps in ovothiol A biosynthesis: C-S lyase and methyltransferase reactions. *Org. Lett.* **20**, 5427–5430 (2018).
31. J. Corradi, C. Bouzat, Understanding the bases of function and modulation of α7 nicotinic receptors: Implications for drug discovery. *Mol. Pharmacol.* **90**, 288–299 (2016).
32. N. Abraham, R. J. Lewis, Neuronal nicotinic acetylcholine receptor modulators from cone snails. *Mar. Drugs* **16**, 208 (2018).
33. R. W. Teichert, E. W. Schmidt, B. M. Olivera, Constellation pharmacology: A new paradigm for drug discovery. *Annu. Rev. Pharmacol. Toxicol.* **55**, 573–589 (2015).
34. E. Monnier, L. Limpalaër, A. Robin, C. Roux, *A Taxonomic Iconography of Living Conidae—Volume 1* (ConchBooks, 2018).
35. E. G. Fofanova, T. D. Mayorova, E. E. Voronezhskaya, Paradoxical effect of sorotonin on ciliary locomotion of the adult archiannelid worms *Dinophilus gyrociliatus* and *D. taeniatus* (Annelida: Polychaeta). *Invert. Zool.* **14**, 114–120 (2017).
36. B. D. Sloley, γ-Glutamyl conjugation of 5-hydroxytryptamine (serotonin) in the earthworm (*Lumbricus terrestris*). *Neurochem. Res.* **19**, 217–222 (1994).
37. A. W. Sangster, S. E. Thomas, N. L. Tingling, Fish attractants from marine invertebrates: Arcamine from *Arca zebra* and strombine from *Strombus gigas*. *Tetrahedron* **31**, 1135–1137 (1974).
38. G. Ortar, M. G. Cascio, L. de Petrocellis, E. Morera, F. Rossi, A. Schiano-Moriello, M. Nalli, V. de Novellis, D. F. Woodward, S. Maione, V. di Marzo, New *N*-arachidonoylserotonin analogues with potential "Dual" mechanism of action against pain. *J. Med. Chem.* **50**, 6554–6569 (2007).
39. A. Fischer, A. Dorresteijn, The polychaete *Platynereis dumerilii* (Annelida): A laboratory animal with spiralian cleavage, lifelong segment proliferation and a mixed benthic/pelagic life cycle. *Bioessays* **26**, 314–325 (2004).
40. W. G. Eberhard, Aggressive chemical mimicry by a bolas spider. *Science* **198**, 1173–1175 (1977).
41. M. K. Stowe, J. H. Tumlinson, R. R. Heath, Chemical mimicry: Bolas spiders emit components of moth prey species sex pheromones. *Science* **236**, 964–967 (1987).
42. C. Gemeno, K. V. Yeargan, K. F. Haynes, Aggressive chemical mimicry by the bolas spider *Mastophora hutchinsoni*: Identification and quantification of a major prey's sex pheromone components in the spider's volatile emissions. *J. Chem. Ecol.* **26**, 1235–1243 (2000).
43. R. R. Jackson, F. R. Cross, A cognitive perspective on aggressive mimicry. *J. Zool.* **290**, 161–171 (2013).
44. G. A. Jamie, Signals, cues and the nature of mimicry. *Proc. Biol. Sci.* **284**, 20162080 (2017).
45. E. Gebel Berg, The chemistry of the pill. *ACS Cent. Sci.* **1**, 5–7 (2015).
46. E. Zeeck, J. Hardege, H. Bartels-Hardege, Sex pheromones and reproductive isolation in two nereid species, *Nereis succinea* and *Platynereis dumerilii*. *Mar. Ecol. Prog. Ser.* **67**, 183–188 (1990).
47. J. Hardege, C. T. Müller, M. Beckmann, H. D. Bartels-Hardege, Timing of reproduction in marine polychaetes: The role of sex pheromones. *Ecoscience* **5**, 395–404 (1998).
48. M. D. Shultz, Two decades under the influence of the rule of five and the changing properties of approved oral drugs. *J. Med. Chem.* **62**, 1701–1714 (2019).
49. Z. Lin, S. Phadke, Z. Lu, S. Beyhan, M. H. Abdel Aziz, C. Reilly, E. W. Schmidt, Onydecalins, fungal polyketides with anti-*Histoplasma* and anti-TRP activity. *J. Nat. Prod.* **81**, 2605–2611 (2018).
50. M. Wang, J. J. Carver, V. V. Phelan, L. M. Sanchez, N. Garg, Y. Peng, D. D. Nguyen, J. Watrous, C. A. Kapono, T. Luzzatto-Knaan, C. Porto, A. Bouslimani, A. V. Melnik, M. J. Meehan, W.-T. Liu, M. Crüsemann, P. D. Boudreau, E. Esquenazi, M. Sandoval-Calderón, R. D. Kersten, L. A. Pace, R. A. Quinn, K. R. Duncan, C.-C. Hsu, D. J. Floros, R. G. Gavilan, K. Kleigrewe, T. Northen, R. J. Dutton, D. Parrot, E. E. Carlson, B. Aigle, C. F. Michelsen, L. Jelsbak, C. Sohlenkamp, P. Pevzner, A. Edlund, J. M. Lean, J. Piel, B. T. Murphy, L. Gerwick, C.-C. Liaw, Y.-L. Yang, H.-U. Humpf, M. Maansson, R. A. Keyzers, A. C. Sims, A. R. Johnson, A. M. Sidebottom, B. E. Sedio, A. Klitgaard, C. B. Larson, C. A. Boya P, D. Torres-Mendoza, D. J. Gonzalez, D. B. Silva, L. M. Marques, D. P. Demarque, E. Pociute, E. C. O'Neill, E. Briand, E. J. N. Helfrich, E. A. Granatosky, E. Glukhov, F. Ryffel, H. Houson, H. Mohimani, J. J. Kharbush, Y. Zeng, J. A. Vorholt, K. L. Kurita, P. Charusanti, K. L. McPhail, K. F. Nielsen, L. Vuong, M. Elfeki, M. F. Traxler, N. Engene, N. Koyama, O. B. Vining, R. Baric, R. R. Silva, S. J. Mascuch, S. Tomasi, S. Jenkins, V. Macherla, T. Hoffman, V. Agarwal, P. G. Williams, J. Dai, R. Neupane, J. Gurr, A. M. C. Rodríguez, A. Lamsa, C. Zhang, K. Dorrestein, B. M. Duggan, J. Almaliti, P.-M. Allard, P. Phapale,

L.-F. Nothias, T. Alexandrov, M. Litaudon, J.-L. Wolfender, J. E. Kyle, T. O. Metz, T. Peryea, D.-T. Nguyen, D. Van Leer, P. Shinn, A. Jadhav, R. Müller, K. M. Waters, W. Shi, X. Liu, L. Zhang, R. Knight, P. R. Jensen, B. Ø. Palsson, K. Pogliano, R. G. Linington, M. Gutiérrez, N. P. Lopes, W. H. Gerwick, B. S. Moore, P. C. Dorrestein, N. Bandeira, Sharing and community curation of mass spectrometry data with Global Natural Products Social Molecular Networking. *Nat. Biotechnol.* **34**, 828–837 (2016).
51. P. Shannon, A. Markiel, O. Ozier, N. S. Baliga, J. T. Wang, D. Ramage, N. Amin, B. Schwikowski, T. Ideker, Cytoscape: A software environment for integrated models of biomolecular interaction networks. *Genome Res.* **13**, 2498–2504 (2003).
52. A. Bankevich, S. Nurk, D. Antipov, A. A. Gurevich, M. Dvorkin, A. S. Kulikov, V. M. Lesin, S. I. Nikolenko, S. Pham, A. D. Prjibelski, A. V. Pyshkin, A. V. Sirotkin, N. Vyahhi, G. Tesler, M. A. Alekseyev, P. A. Pevzner, SPAdes: A new genome assembly algorithm and its applications to single-cell sequencing. *J. Comput. Biol.* **19**, 455–477 (2012).
53. D. Hyatt, G.-L. Chen, P. F. LoCascio, M. L. Land, F. W. Larimer, L. J. Hauser, Prodigal: Prokaryotic gene recognition and translation initiation site identification. *BMC Bioinformatics* **11**, 119 (2010).
54. B. Langmead, C. Trapnell, M. Pop, S. L. Salzberg, Ultrafast and memory-efficient alignment of short DNA sequences to the human genome. *Genome Biol.* **10**, R25 (2009).
55. N. M. Davidson, A. Oshlack, Corset: Enabling differential gene expression analysis for *de novo*assembled transcriptomes. *Genome Biol.* **15**, 410 (2014).
56. M. D. Robinson, D. J. McCarthy, G. K. Smyth, edgeR: A Bioconductor package for differential expression analysis of digital gene expression data. *Bioinformatics* **26**, 139–140 (2010).
57. O. Folmer, M. Black, W. Hoeh, R. Lutz, R. Vrijenhoek, DNA primers for amplification of mitochondrial cytochrome c oxidase subunit I from diverse metazoan invertebrates. *Mol. Mar. Biol. Biotechnol.* **3**, 294–299 (1994).
58. M. A. Larkin, G. Blackshields, N. P. Brown, R. Chenna, P. A. McGettigan, H. McWilliam, F. Valentin, I. M. Wallace, A. Wilm, R. Lopez, J. D. Thompson, T. J. Gibson, D. G. Higgins, Clustal W and Clustal X version 2.0. *Bioinformatics* **23**, 2947–2948 (2007).
59. A. Dereeper, V. Guignon, G. Blanc, S. Audic, S. Buffet, F. Chevenet, J.-F. Dufayard, S. Guindon, V. Lefort, M. Lescot, J.-M. Claverie, O. Gascuel, Phylogeny.fr: Robust phylogenetic analysis for the non-specialist. *Nucleic Acids Res.* **36**, W465–W469 (2008).
60. R. W. Teichert, N. J. Smith, S. Raghuraman, D. Yoshikami, A. R. Light, B. M. Olivera, Functional profiling of neurons through cellular neuropharmacology. *Proc. Natl. Acad. Sci. U.S.A.* **109**, 1388–1395 (2012).
61. M. J. Giacobassi, L. S. Leavitt, S. Raghuraman, R. Alluri, K. Chase, R. K. Finol-Urdaneta, H. Terlau, R. W. Teichert, B. M. Olivera, An integrative approach to the facile functional classification of dorsal root ganglion neuronal subclasses. *Proc. Natl. Acad. Sci. U.S.A.* **117**, 5494–5501 (2020).
62. H. Gross, J. Reitner, G. M. König, Isolation and structure elucidation of azoricasterol, a new sterol of the deepwater sponge *Macandrewia azorica*. *Naturwissenschaften* **91**, 441–446 (2004).
63. C. D. Smith, A. Wang, K. Vembaiyan, J. Zhang, C. Xie, Q. Zhou, G. Wu, S. R. W. Chen, T. G. Back, Novel carvedilol analogues that suppress store-overload-induced Ca^{2+} release. *J. Med. Chem.* **56**, 8626–8655 (2013).
64. H.-C. Chou, N. Acevedo-Luna, J. A. Kuhlman, S. Q. Schneider, PdumBase: A transcriptome database and research tool for *Platynereis dumerilii* and early development of other metazoans. *BMC Genomics* **19**, 618 (2018).
65. J. S. Biggs, M. Watkins, N. Puillandre, J. P. Ownby, E. Lopez-Vera, S. Christensen, K. J. Moreno, J. Bernaldez, A. Licea-Navarro, P. S. Corneli, B. M. Olivera, Evolution of *Conus* peptide toxins: Analysis of *Conus californicus* Reeve, 1844. *Mol. Phylogenet. Evol.* **56**, 1–12 (2010).
66. S. Albade, M. J. Tenorio, C. M. L. Afonso, J. E. Uribe, A. M. Echeverry, R. Zardoya, Phylogenetic relationships of cone snails endemic to Cabo Verde based on mitochondrial genomes. *BMC Evol. Biol.* **17**, 231 (2017).
67. M. J. Tenorio, S. Abalde, J. R. Pardos-Blas, R. Zardoya, Taxonomic revision of West African cone snails (Gastropoda: Conidae) based upon mitogenomic studies: Implications for conservation. *Eur. J. Taxon.* **663**, 1–89 (2020).
68. T. F. Duda Jr., E. Rolán, Explosive radiation of Cape Verde *Conus*, a marine species flock. *Mol. Ecol.* **14**, 267–272 (2005).
69. M. J. Tenorio, S. Abalde, R. Zardoya, Identification of new species of *Kalloconus* and *Africonus* (Gastropoda, Conidae) from the Cabo Verde Islands through mitochondrial genome comparison. *Festivus* **50**, 73–88 (2018).
70. M. Watkins, P. S. Cornell, D. Hillyard, B. M. Olivera, Molecular phylogeny of *Conus chiangi* (Azuma, 1972) (Gastropoda: Conidae). *Nautilus* **124**, 129–136 (2010).
71. S. Albade, M. J. Tenorio, J. E. Uribe, R. Zardoya, Conidae phylogenomics and evolution. *Zool. Scr.* **48**, 119–214 (2019).

Acknowledgments: We thank J. L. B. Neves for providing *C. genuanus*. We thank S. B. Christensen for dissecting some of the cone snail used in this work. Work in the Philippines was completed thanks to supervision of the Department of Agriculture–Bureau of Fisheries and Aquatic Resources, Philippines (DA-BFAR). **Funding:** Research reported in this publication was supported by NIH R35GM12252, with contributions to biological work from NIH Fogarty International Center U19TW008163, NIH P01GM48677, and DOD CDMRP W81XWH-17-1-0413. The content is solely the responsibility of the authors and does not necessarily represent the official views of the NIH. **Author contributions:** J.P.T. conceived and performed the ecology and biosynthesis experiments. Z.L. discovered the compounds and chemically characterized them. Z.L., J.P.T., and H.S.-H. performed transcriptomic experiments and analyses. M.W. performed phylogenetic analysis. P.F.S. and R.P.B. created Ruby-Tracker. S.E. improved data analysis of ecological experiments. Y.F. synthesized compounds needed for biosynthetic studies. J.R.M., and R.K.F.-U. performed electrophysiological screening on mammalian ion channels. H.-S.T. performed α7 recordings. J.T. performed DRG assays. A.A.Y. and N.S. facilitated snail collections. Amphinomid assays in the Philippines were run in the laboratory of G.P.C. D.T. set up and recorded *C. imperialis* movies. B.D.Ö. led polychaete worm experiments. B.M.O. and E.W.S. led the research. J.P.T., Z.L., and E.W.S. wrote the manuscript. **Competing interests:** The authors declare that they have no competing interests. **Data and materials availability:** All data needed to evaluate the conclusions in the paper are present in the paper and/or the Supplementary Materials. LC-MS data are available at the Center for Computational Mass Spectrometry with MassIVE MSV000085600. GenBank accession numbers are available for all COI genes (see table S4), for *conA* (MW513375), and for *C. imperialis* transcriptomes shown in fig. S2A (SAMN15495218, SAMN15495219, AMN15495220, SAMN15495221, SAMN15495222, and SAMN15495223 under bioproject PRJNA645157). Additional data and materials will be provided by request to corresponding authors.

Submitted 14 October 2020
Accepted 26 January 2021
Published 12 March 2021
10.1126/sciadv.abf2704

Citation: J. P. Torres, Z. Lin, M. Watkins, P. F. Salcedo, R. P. Baskin, S. Elhabian, H. Safavi-Hemami, D. Taylor, J. Tun, G. P. Concepcion, N. Saguil, A. A. Yanagihara, Y. Fang, J. R. McArthur, H.-S. Tae, R. K. Finol-Urdaneta, B. D. Özpolat, B. M. Olivera, E. W. Schmidt, Small-molecule mimicry hunting strategy in the imperial cone snail, *Conus imperialis*. *Sci. Adv.* **7**, eabf2704 (2021).

Science Advances

Small-molecule mimicry hunting strategy in the imperial cone snail, *Conus imperialis*

Joshua P. Torres, Zhenjian Lin, Maren Watkins, Paula Flórez Salcedo, Robert P. Baskin, Shireen Elhabian, Helena Safavi-Hemami, Dylan Taylor, Jortan Tun, Gisela P. Concepcion, Noel Saguil, Angel A. Yanagihara, Yixin Fang, Jeffrey R. McArthur, Han-Shen Tae, Rocio K. Finol-Urdaneta, B. Duygu Özpolat, Baldomero M. Olivera and Eric W. Schmidt

Sci Adv **7** (11), eabf2704.
DOI: 10.1126/sciadv.abf2704